PAPER

Chaotic behavior, bifurcations, sensitivity analysis, and novel optical soliton solutions to the Hamiltonian amplitude equation in optical physics

Physica Scripta

PAPER

Chaotic behavior, bifurcations, sensitivity analysis, and novel optical soliton solutions to the Hamiltonian amplitude equation in optical physics

RECEIVED
21 March 2024

REVISED
13 May 2024

ACCEPTED FOR PUBLICATION
31 May 2024

PUBLISHED
12 June 2024

Md Nur Hossain[1,2], **M Mamun Miah**[3,4,*], **Faisal Z Duraihem**[5], **Sadique Rehman**[3] and **Wen-Xiu Ma**[6,7,8,*]

[1] Graduate School of Engineering, Osaka University, Osaka, 5650871, Japan
[2] Department of Mathematics, Dhaka University of Engineering & Technology, Gazipur-1707, Bangladesh
[3] Division of Mathematical and Physical Sciences, Kanazawa University, Kanazawa-9201192, Japan
[4] Department of Mathematics, Khulna University of Engineering & Technology, Khulna-9203, Bangladesh
[5] Department of Mathematics, College of Science, King Saud University, Riyadh, 11451, Saudi Arabia
[6] Department of Mathematics, Zhejiang Normal University, Jinhua, 321004, Zhejiang, People's Republic of China
[7] Department of Mathematics and Statistics, University of South Florida, Tampa, FL, 33620-5700, United States of America
[8] Material Science Innovation and Modelling, Department of Mathematical Sciences, North-West University, Mafikeng Campus, Mmabatho 2735, South Africa
[*] Authors to whom any correspondence should be addressed.

E-mail: mawx@cas.usf.edu **and** mamun0954@stu.kanazawa-u.ac.jp

Abstract

This study, highlights the exact optical soliton solutions in the context of optical physics, centering on the intricate Hamiltonian amplitude equation with bifurcation and sensitivity analysis. This equation is pivotal in optics which underpins the understanding of optical manifestations, encompassing solitons, nonlinear consequences, and wave interactions. Applying an analytical expansion approach, we extract diverse optical solutions, having trigonometric, hyperbolic, and rational functions. Next, we utilize concepts from the principle of planar dynamical systems to investigate the bifurcation processes and chaotic behaviors present in this derived system. Additionally, we use the Runge–Kutta scheme to carry out a thorough sensitivity analysis of the dynamical system. It has been verified through this analytical process that small variations in beginning conditions have negligible effects on the stability of the solution using bifurcation analysis. Validation via Mathematica software ensures the accuracy of these findings. Furthermore, we employ dynamic visualizations, such as 2D, 3D, and contour plots, to illustrate various soliton patterns, including kink, multi-kink, single periodic, multi-periodic, singular, and semi-bell-shaped configurations. These visual representations provide a glimpse into the fascinating behavior of optical phenomena. The solutions obtained via this proposed method showcase its efficacy, dependability, and simplicity in comparison to various alternative approaches.

1. Introduction

The study of optical solitons offers a captivating avenue of exploration, especially when delving into the subtleties of soliton transmission within optical fibers and the intricate interactions between intense laser radiation and plasmas. Additionally, solitons are vital for maintaining minimal distortion during long-distance data transmission in optical fiber communications, crucial for high-speed telecommunications networks. They also play a pivotal role in nonlinear optical devices, enabling precise signal manipulation and processing, particularly in optical switches, modulators, and amplifiers (Manafian 2016, Biswas 2018, Tariq *et al* 2018, Hossain *et al* 2024b). The Hamiltonian amplitude equation (HAE), a multifaceted nonlinear partial differential equation extensively used in optics, serves as a fundamental mathematical tool (Wadati *et al* 1992). It is extremely important for simulating a wide variety of optical phenomena, including wave propagation, optical solitons generation, and complex nonlinear phenomena in optical fibers and related instruments. Researchers highly prioritize HAE because it illuminates the dynamics of optical waves across various scenarios. These

scenarios encompass the generation of advanced optical solitons, the discovery of interactions among optical waves, and the analysis of how light pulses propagate through nonlinear optical materials. Within the field of optics, the study of the HAE assumes paramount importance, especially when it comes to designing and evaluating optical systems and equipment. Its relevance extends to critical domains such as laser technology and optical communication networks, where nonlinear effects and wave interactions wield substantial influence.

To uncover exact solutions for different nonlinear equations (NLEs) like HAE, researchers employ several methods including the unified method (Fokas and Lenells 2012, Abdel-Gawad and Osman 2015), the transformed rational function method (Ma and Lee 2009) the extended direct algebraic method (Gao *et al* 2020, Shahzad *et al* 2023), Lie group method (Buckwar and Luchko 1998, Jafari *et al* 2015), Hirota's bilinear method (Zhou *et al* 2006, Liu *et al* 2019), the $\exp(-\varphi(\xi))$-expansion method (Roshid *et al* 2014, Raza *et al* 2019), the generalized Kudryshov method (Islam *et al* 2015, Habib *et al* 2019), the variational iteration method (Abdel-Gawad and Osman 2013, Seadawy 2015), the Backlund transform method (Yuan *et al* 2011), the sine–Gordon expansion method (Kumar *et al* 2017, Ali *et al* 2020), the Cole–Hopf transformation method (Salas and Gmez S 2010), the auxiliary equation method (Zhang 2013, Islam *et al* 2023), the homotopy-perturbation method (Cveticanin 2006), the tanh–function method (Parkes and Duffy 1996, Fan 2000), homogeneous balance method (Wang *et al* 1996, Fan and Zhang 1998), Hirota bilinear formulation with N- soliton (Ma 2020 2021), the $(\dot{G}/G)$-expansion method (Wang *et al* 2008, Zayed and Gepreel 2009, Khan *et al* 2023), the fractional approach (Tandel *et al* 2022), the (G'/G^2)-expansion method (Islam *et al* 2022), multiple exp-function method (Ma *et al* 2010, Ma and Zhu 2012), the tanh–coth method (Kumar and Pankaj 2015, Mamun *et al* 2022) and many others.

Recently, some researchers (Teh *et al* 1997, Yomba 2005, Taghizadeh and Mirzazadeh 2011, Bekir and San 2012, Kumar *et al* 2012, Mirzazadeh 2014, 2015) have investigated the behavior of the HAE through some methodologies such as the Riccati equation approach, He's semi-inverse method combined with the ansatz approach, the first integral technique, the modified simple equation method, the functional variable approach, the Jacobi elliptic function method, the Lie classical method, and the $(\dot{G}/G)$-expansion approach.

Although these methods have succeeded in deriving exact solutions for the HAE, the majority of these methods rely on single-variable approaches, resulting in nearly identical solutions. To address this limitation, we aim to employ a highly valuable and beneficial technique known as the double $(\dot{G}/G, 1/G)$-expansion method, which was extensively utilized to unveil exact solutions of several physical models by numerous researchers (Zayed and Alurrfi 2014, Inan *et al* 2015, Miah *et al* 2017, Akher Chowdhury *et al* 2021, Akbar *et al* 2023, Ali *et al* 2023, Iqbal *et al* 2023, Mohanty *et al* 2023, Vivas-Cortez *et al* 2023, Hossain *et al* 2024a). This method centers on expressing solutions as power series, where the coefficients are determined via two variables, $\dot{G}/G$ and $1/G$. The approach involves determining these coefficients inserting the series into the equation and then similar coefficients of similar terms. Nevertheless, no one has investigated optical solutions utilizing the $(\dot{G}/G, 1/G)$-expansion approach for the HAE up to this point. This study aims to derive optical soliton solutions for HAE using the $(\dot{G}/G, 1/G)$ expansion approach. The paper is organized as follows: (i) section 2 presents an overview of the methodology utilized, (ii) section 3 applies the $(\dot{G}/G, 1/G)$ expansion approach to the HAE and derives the necessary solutions, (iii) section 4 illustrates the bifurcation analysis for HAE, while section 5 offers a sensitivity analysis for the stability of solutions, (iv) section 6 delves into the examination of dynamic depictions, highlighting the fascinating behaviors of various solidarities via 3D, 2D, and contour displays, (v) Finishing remarks are provided in section 7, followed by a list of references in the concluding section.

2. Discussion about the method $(\dot{G}/G, \quad 1/G$- expansion scheme)

This section presents the essential procedures for using the two variables $(\dot{G}/G, 1/G)$-expansion approach to the analysis of the NLEs (Rasid *et al* 2023, Yue *et al* 2023). To facilitate the derivation of exact solutions, this method introduces a linear ordinary differential equation, expressed as follows:

$$\ddot{G}(\zeta) + \lambda G(\zeta) = \alpha, \tag{1}$$

where the symbol '.' stands for the differentiation concerning ζ and the variables might correspond to as follows:

$$Q = \frac{\dot{G}(\zeta)}{G(\zeta)}, \text{ and } R = \frac{1}{G(\zeta)}. \tag{2}$$

It is supplied the subsequent relationships as:

$$\dot{Q} = -Q^2 + \alpha R - \lambda, \quad \text{and} \quad \dot{R} = -QR, \tag{3}$$

where Q and R is the function of ζ.

The outcome of equation (1) mentioned above depends on λ and can be categorized as follows:

***Instance*1**: When λ is positive.

The general solution (GS) of equation (1) for this case can be represented in the following manner:

$$G(\zeta) = C\sin(\zeta\sqrt{\lambda}) + D\cos(\zeta\sqrt{\lambda}) + \alpha/\lambda, \tag{4}$$

which yields

$$R^2 = \left(\frac{Q^2 - 2\alpha R + \lambda}{A\lambda^2 - \alpha^2}\right)\lambda, \tag{5}$$

where $A = C^2 + D^2$ stands for the subtraction of the squares of arbitrary constants C and D.

***Instance*2**: When λ is negative.

The GS of equation (1) for this case can be expressed as follows:

$$G(\zeta) = C\sin h(\zeta\sqrt{-\lambda}) + D\cos h(\zeta\sqrt{-\lambda}) + \alpha/\lambda, \tag{6}$$

resulting in:

$$R^2 = -\lambda\left(\frac{Q^2 - 2\alpha R + \lambda}{B\lambda^2 + \alpha^2}\right), \tag{7}$$

where $B = C^2 - D^2$ stands for the sum of the squares of arbitrary constants C and D.

***Instance*3**: When λ is equal to zero.

For this case, equation (1) yields the GS as follows:

$$G(\zeta) = \frac{\alpha\zeta^2}{2} + C\zeta + D, \tag{8}$$

which provides:

$$R^2 = \left(\frac{Q^2 - 2\alpha R}{C^2 - 2\alpha D}\right). \tag{9}$$

Let us now assume that the general representation of NLEs with three variables (x, y, and t) is as follows:

$$S(\mathcal{H}, \mathcal{H}_x, \mathcal{H}_{xx}, \mathcal{H}_y, \mathcal{H}_{yy}, \mathcal{H}_{xy}, \mathcal{H}_t, \mathcal{H}_{tt}, \mathcal{H}_{xt}, \ldots\ldots\ldots) = 0. \tag{10}$$

In this context, S is a polynomial function that depends on the variables $\mathcal{H}$ and $\mathcal{H}_x = \frac{\partial\mathcal{H}}{\partial x}$, $\mathcal{H}_y = \frac{\partial\mathcal{H}}{\partial y}$, $\mathcal{H}_t = \frac{\partial\mathcal{H}}{\partial t}$, $\mathcal{H}_{xx} = \frac{\partial^2\mathcal{H}}{\partial x^2}$, $\mathcal{H}_{yy} = \frac{\partial^2\mathcal{H}}{\partial y^2}$, $\mathcal{H}_{tt} = \frac{\partial^2\mathcal{H}}{\partial t^2}$, $\mathcal{H}_{xt} = \frac{\partial\mathcal{H}}{\partial x\partial t}$, $\mathcal{H}_{xy} = \frac{\partial\mathcal{H}}{\partial x\partial y}$ and so on.

To transform this equation, introduce a new wave variable ζ with the following relationships:

$$\mathcal{H}(x, t) = e^{i\eta}\mathcal{H}(\zeta), \quad \eta = dx - \beta t, \quad \text{and} \quad \zeta = \mu(x - bt). \tag{11}$$

Applying this transformation to equation (10) yields:

$$T(\mathcal{H}, \dot{\mathcal{H}}, \ddot{\mathcal{H}}, \dddot{\mathcal{H}}, \ldots\ldots\ldots) = 0. \tag{12}$$

In this context, T denotes the polynomial incorporating $\mathcal{H}$ and its ordinary derivatives.

Let us consider the GS of equation (12) as follows:

$$\mathcal{H}(\zeta) = a_0 + \sum_{j=1}^{M} a_j Q^j(\zeta) + \sum_{j=1}^{M} b_j Q^{j-1}(\zeta)R(\zeta) \tag{13}$$

where a_0, a_j, and b_j ($j = 1, \quad 2, \quad 3, \ldots\ldots\ldots, M$) are the unknown coefficients satisfying the condition $a_M^2 + b_M^2 \neq 0$ and the parameter M is the balanced number, and it is always positive. Now, we need to find these arbitrary constants (a_0, a_j and b_j) using the above-mentioned method with the subsequent steps:

Step I: Applying the homogeneous balance method to obtain the balance number M (Miah *et al* 2017).

Step II: By substituting the value of M into equation (13) and later replacing this in equation (12), by employing equations (3) and (5) (for instance I), the left-hand side of equation (12) transforms a polynomial that encompasses Q and R. In this polynomial, the degree attributed to R does not exceed *1*, and the degree of Q varies from zero to any number (integer). Equating the coefficients of each term with similar powers results in a set of algebraic equations that involves the variables a_j (for $j = 0, 1, 2, \ldots, M$), b_j (for $j = 1, 2, 3, \ldots, M$), λ (where $\lambda > 0$), α.

Step III: Then solving the set of equations found in step II, we figure out the values of a_j, b_j, λ (where $\lambda > 0$), and α. Subsequently, by substituting these values, along with a_j (for $j = 0, 1, 2, \ldots, M$), b_j (for $j = 0, 1, 2, \ldots, M$), λ, and α into the transformed equation (13), we can derive the optical solutions in terms of trigonometric functions. Ultimately, this process yields the optical solution of the desired HAE.

Step IV: Apply analogous methodologies as outlined in sections I and II, which yield precise solutions expressed in terms of hyperbolic and rational functions, providing further insights into (Miah *et al* 2020, Rasid *et al* 2023, Yue *et al* 2023)

3. Applications of the method

In this portion, we utilize the above-mentioned technique to perform an analytical analysis of the HAE as outlined in the reference (Zafar *et al* 2020). The nonlinear complex form of this equation is as follows:

$$i\mathcal{H}_x + \mathcal{H}_{tt} + 2\kappa\,|\mathcal{H}|^2\mathcal{H} - \varepsilon\mathcal{H}_{xt} = 0, \quad \kappa = \pm 1, \tag{14}$$

where 'i' is the imaginary unit ($i = \sqrt{-1}$), and $\mathcal{H}(x, t)$ signifies the complex function. However, the last term of equation (14) indicates that the nonlinear Schrödinger equation exhibits ill-posed behavior.

Now, using the transformation outlined in equations (11), and (14) into the following ordinary differential format:

$$\mu^2(b^2 + \epsilon\, b)\ddot{\mathscr{H}} - (d + \beta^2 + d\epsilon\beta)\mathscr{H} + 2\kappa\mathcal{H}^3 = 0, \text{ (real part)} \tag{15}$$

and

$$(1 + bd\varepsilon + \beta\epsilon + 2b\beta)\dot{\mathcal{H}} = 0. \text{ (imaginary part)} \tag{16}$$

Applying the balancing principle, we found the value of M was 1. With this balance number, we can express the GS of equation (15) as follows:

$$\mathcal{H}(\zeta) = a_0 + a_1 Q(\zeta) + b_1 R(\zeta), \tag{17}$$

where a_0, a_1, and b_1 are unknown coefficients that require to be determined.

Subsequently, we implemented the three distinct cases as outlined in section 2.

Instance I: $\lambda > 0$ (For trigonometric solutions)

The necessary solution can be obtained by substituting equation (17) into equation (16) and applying equations (2) and (3), and changing the left side of equation (16) to a polynomial that includes Q and R. The coefficients a_0, a_1, b_1, α, λ and d are involved in a set of algebraic equations that are obtained by equating eachs coefficient of this polynomial to zero. After solving these algebraic systems, the arbitrary constants take on the following values:

$$a_0 = 0, \quad a_1 = \pm\frac{\mu\sqrt{-b}\,\sqrt{b+\varepsilon}}{2\sqrt{\kappa}}, \quad b_1 = \pm\frac{\mu\sqrt{-b}\,\sqrt{b+\varepsilon}\,\sqrt{-\alpha^2 + A\lambda^2}}{2\sqrt{\kappa}\,\sqrt{\lambda}},$$
$$\text{and} \quad d = \frac{-2\beta^2 + b^2\lambda\mu^2 + b\epsilon\lambda\mu^2}{2(1+\epsilon\beta)} \tag{18}$$

Now, using these values in equation (17), which yields:

$$\mathscr{H}(\zeta) = \pm\frac{\mu\sqrt{-b}\,\sqrt{b+\varepsilon}}{2\sqrt{\kappa}}\sqrt{\lambda}\,\frac{(C\cos(\zeta\sqrt{\lambda}) - D\sin(\zeta\sqrt{\lambda}))}{C\sin(\zeta\sqrt{\lambda}) + D\cos(\zeta\sqrt{\lambda}) + \alpha/\lambda}$$
$$\pm\frac{\mu\sqrt{-b}\,\sqrt{b+\varepsilon}\,\sqrt{-\alpha^2 + A\lambda^2}}{2\sqrt{\kappa}\,\sqrt{\lambda}}\,\frac{1}{C\sin(\zeta\sqrt{\lambda}) + D\cos(\zeta\sqrt{\lambda}) + \alpha/\lambda}, \tag{19}$$

where $b < 0$ and $b + \varepsilon > 0$.

Upon restoring equation (19) to its first form using equation (11), yields:

$$\mathcal{H}(x, t) = e^{i\left(\left(\frac{-2\beta^2 + b^2\lambda\mu^2 + b\epsilon\lambda\mu^2}{2(1+\epsilon\beta)}\right)x - \beta t\right)}$$
$$\left(\pm\frac{\mu\sqrt{-b}\,\sqrt{b+\varepsilon}}{2\sqrt{\kappa}}\sqrt{\lambda}\,\frac{(C\cos(\mu(x-bt)\sqrt{\lambda}) - D\sin(\mu(x-bt)\sqrt{\lambda}))}{C\sin(\mu(x-bt)\sqrt{\lambda}) + D\cos(\mu(x-bt)\sqrt{\lambda}) + \alpha/\lambda}\right.$$
$$\left.\pm\frac{\mu\sqrt{-b}\,\sqrt{b+\varepsilon}\,\sqrt{-\alpha^2 + A\lambda^2}}{2\sqrt{\kappa}\,\sqrt{\lambda}}\,\frac{1}{C\sin(\mu(x-bt)\sqrt{\lambda}) + D\cos(\mu(x-bt)\sqrt{\lambda}) + \alpha/\lambda}\right), \tag{20}$$

where $b < 0$ and $b + \varepsilon > 0$.

In particular, when both α and D are equal to zero, but C is not equal to zero, equation (20) yields:

$$\mathcal{H}(x, t) = e^{i\left(\left(\frac{-2\beta^2 + b^2\lambda\mu^2 + b\epsilon\lambda\mu^2}{2(1+\epsilon\beta)}\right)x - \beta t\right)}\left(\pm\frac{\mu\sqrt{-b}\,\sqrt{b+\varepsilon}}{2\sqrt{\kappa}}\sqrt{\lambda}\cot(\mu(x-bt)\sqrt{\lambda})\right.$$

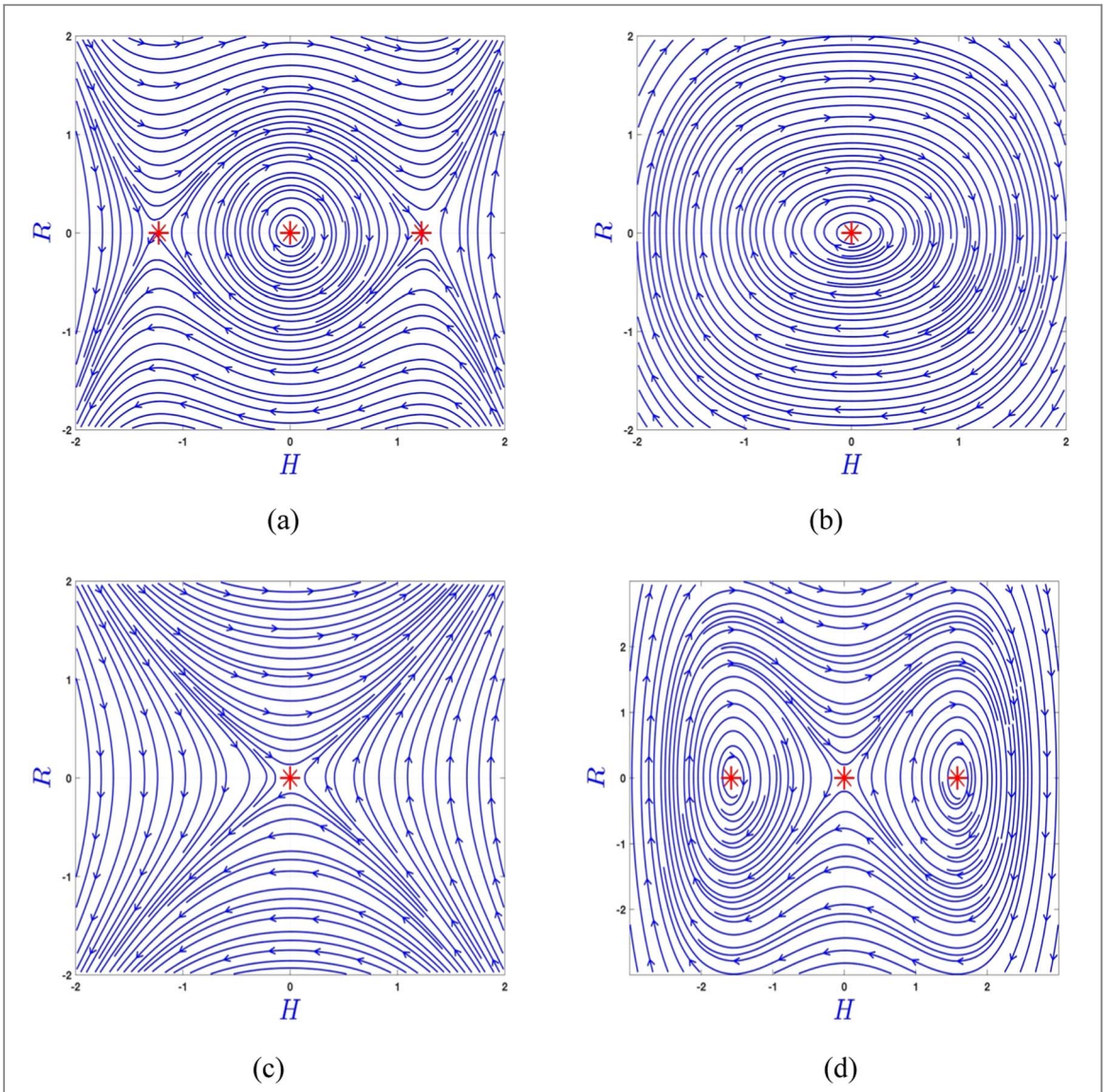

Figure 1. Phase diagrams showing the bifurcations of the suggested system under different conditions for w_1 and w_2: (a) $w_1 > 0$ and $w_2 < 0$, (b) $w_1 < 0$ and $w_2 < 0$, (c) $w_1 > 0$ and $w_2 > 0$, (d) $w_1 < 0$ and $w_2 > 0$, depending on various parameter values.

$$\pm\frac{\mu\sqrt{-b}\quad\sqrt{b+\varepsilon}\,\lambda}{2\sqrt{\kappa}\,\sqrt{\lambda}}\mathrm{cosec}(\mu(x-bt)\sqrt{\lambda})\Bigg), \tag{21}$$

where $b < 0$ and $b + \varepsilon > 0$.

Similarly, if both α and C to zero but D is not equal to zero, equation (20) yields:

$$\mathscr{H}(x,t) = e^{i\left(\left(\frac{-2\beta^2+b^2\lambda\mu^2+b\epsilon\lambda\mu^2}{2(1+\epsilon\beta)}\right)x-\beta t\right)}\Bigg(\pm\frac{\mu\sqrt{-b}\quad\sqrt{b+\varepsilon}}{2\sqrt{\kappa}}\sqrt{\lambda}\tan(\mu(x-bt)\sqrt{\lambda})$$

$$\pm\frac{\mu\sqrt{-b}\quad\sqrt{b+\varepsilon}\,\lambda}{2\sqrt{\kappa}\,\sqrt{\lambda}}\sec(\mu(x-bt)\sqrt{\lambda})\Bigg), \tag{22}$$

where $b < 0$ and $b + \varepsilon > 0$.

Instance II: $\lambda < 0$ (For hyperbolic solutions)

Similarly, we follow the procedure outlined in instance I to determine the coefficients' values, leading to the following results:

$$a_0 = 0, \quad a_1 = \pm\frac{\mu\sqrt{-b}\quad\sqrt{b+\varepsilon}}{2\sqrt{\kappa}}, b_1 = \pm\frac{\mu\sqrt{-b}\quad\sqrt{b+\varepsilon}\quad\sqrt{\alpha^2+B\lambda^2}}{2\sqrt{\kappa}\,\sqrt{-\lambda}},$$

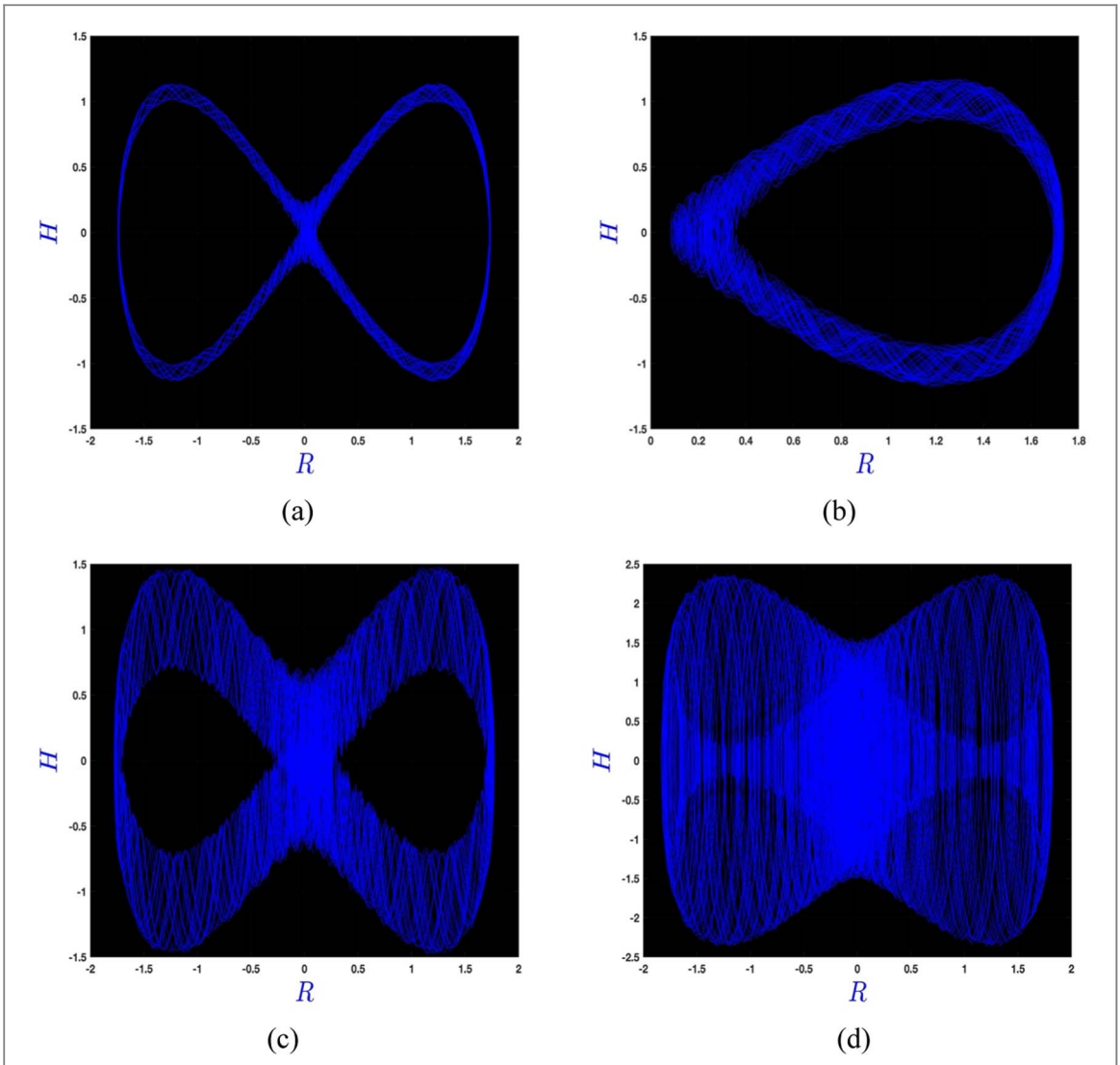

Figure 2. 2D visualizations of chaotic motion for equation (32) with different parameter values as: (a) $\alpha = 1$ and $\theta = \pi/2$, (b) $\alpha = 2$ and $\theta = \pi/2$, (c) $\alpha = 6$ and $\theta = \pi/2$, (d) $\alpha = 20$ and $\theta = \pi/2$.

$$\text{and } d = \frac{-2\beta^2 + b^2\lambda\mu^2 + b\epsilon\lambda\mu^2}{2(1 + \epsilon\beta)}. \tag{23}$$

Using these in equation (17), yields:

$$\mathcal{H}(\zeta) = \pm\frac{\mu\sqrt{-b}\ \sqrt{b+\varepsilon}}{2\sqrt{\kappa}}\sqrt{-\lambda}\,\frac{(C\cosh(\zeta\sqrt{-\lambda}) + D\sinh(\zeta\sqrt{-\lambda}))}{C\sinh(\zeta\sqrt{-\lambda}) + D\cosh(\zeta\sqrt{-\lambda}) + \alpha/\lambda}$$
$$\pm\frac{\mu\sqrt{-b}\ \sqrt{b+\varepsilon}\ \sqrt{\alpha^2 + B\lambda^2}}{2\sqrt{\kappa}\sqrt{-\lambda}}\,\frac{1}{C\sinh(\zeta\sqrt{-\lambda}) + D\cosh(\zeta\sqrt{-\lambda}) + \alpha/\lambda}, \tag{24}$$

where $b < 0$ and $b + \varepsilon > 0$.

Going back to its initial form using transformation variables, we obtain:

$$\mathcal{H}(x,\,t) = e^{i\left(\left(\frac{-2\beta^2 + b^2\lambda\mu^2 + b\epsilon\lambda\mu^2}{2(1+\epsilon\beta)}\right)x - \beta t\right)}$$
$$\left(\pm\frac{\mu\sqrt{-b}\ \sqrt{b+\varepsilon}}{2\sqrt{\kappa}}\sqrt{-\lambda}\,\frac{(C\cosh(\mu(x-bt)\sqrt{-\lambda}) + D\sinh(\mu(x-bt)\sqrt{-\lambda}))}{C\sinh(\mu(x-bt)\sqrt{-\lambda}) + D\cosh(\mu(x-bt)\sqrt{-\lambda}) + \alpha/\lambda}\right.$$
$$\left.\pm\frac{\mu\sqrt{-b}\ \sqrt{b+\varepsilon}\ \sqrt{\alpha^2 + B\lambda^2}}{2\sqrt{\kappa}\sqrt{-\lambda}}\,\frac{1}{C\sinh(\mu(x-bt)\sqrt{-\lambda}) + D\cosh(\mu(x-bt)\sqrt{-\lambda}) + \alpha/\lambda}\right), \tag{25}$$

where $b < 0$ and $b + \varepsilon > 0$.

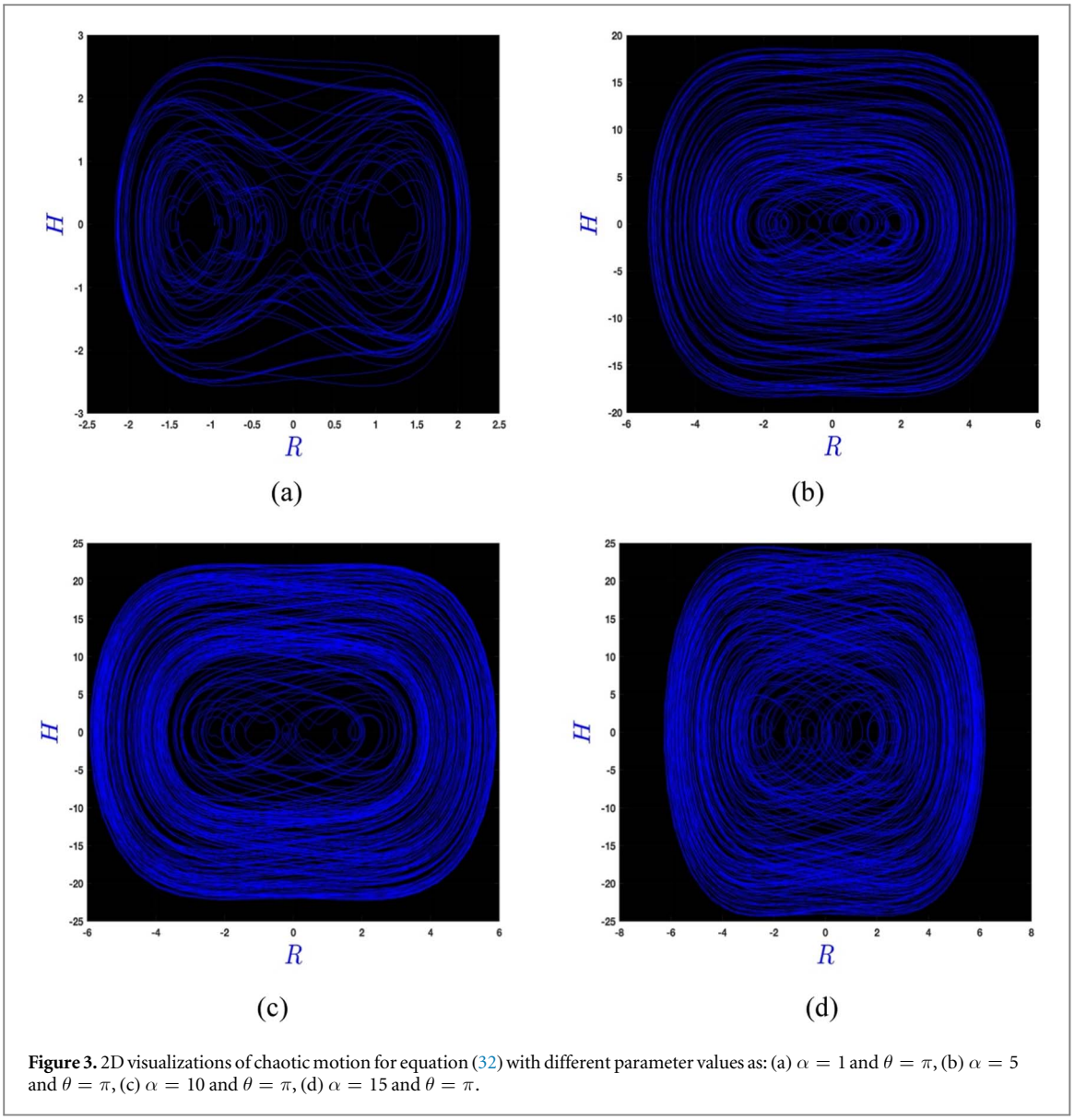

Figure 3. 2D visualizations of chaotic motion for equation (32) with different parameter values as: (a) $\alpha = 1$ and $\theta = \pi$, (b) $\alpha = 5$ and $\theta = \pi$, (c) $\alpha = 10$ and $\theta = \pi$, (d) $\alpha = 15$ and $\theta = \pi$.

When α and D are both set to zero, but C is not equal to zero, equation (25) simplifies as follows:

$$\mathcal{H}(x,\,t) = e^{i\left(\left(\frac{-2\beta^2+b^2\lambda\mu^2+b\epsilon\lambda\mu^2}{2(1+\epsilon\beta)}\right)x-\beta t\right)}$$
$$\left(\pm\frac{\mu\sqrt{-b}\ \sqrt{b+\varepsilon}}{2\sqrt{\kappa}}\sqrt{-\lambda}\,\coth(\mu(x-bt)\sqrt{-\lambda})\right.$$
$$\left.\pm\frac{\mu\sqrt{-b}\ \ \sqrt{b+\varepsilon}\ \ \sqrt{\lambda^2}}{2\sqrt{\kappa}\,\sqrt{-\lambda}}\mathrm{cosech}(\mu(x-bt)\sqrt{-\lambda})\right), \tag{26}$$

where $b < 0$ and $b + \varepsilon > 0$.

Instance III: $\lambda = 0$ (For rational solutions)

Once more, we adhere to the procedure delineated in instance I to deduce the coefficients' values, resulting in the following outcomes:

$$a_0 = 0, \quad a_1 = \pm\frac{\mu\sqrt{-b}\ \sqrt{b+\varepsilon}}{2\sqrt{\kappa}},\ b_1 = \pm\frac{\mu\sqrt{-b}\ \ \sqrt{b+\varepsilon}\ \ \sqrt{C^2-2\alpha D}}{2\sqrt{\kappa}},$$
$$\text{and}\ \ d = \frac{-\beta^2}{(1+\epsilon\beta)}. \tag{27}$$

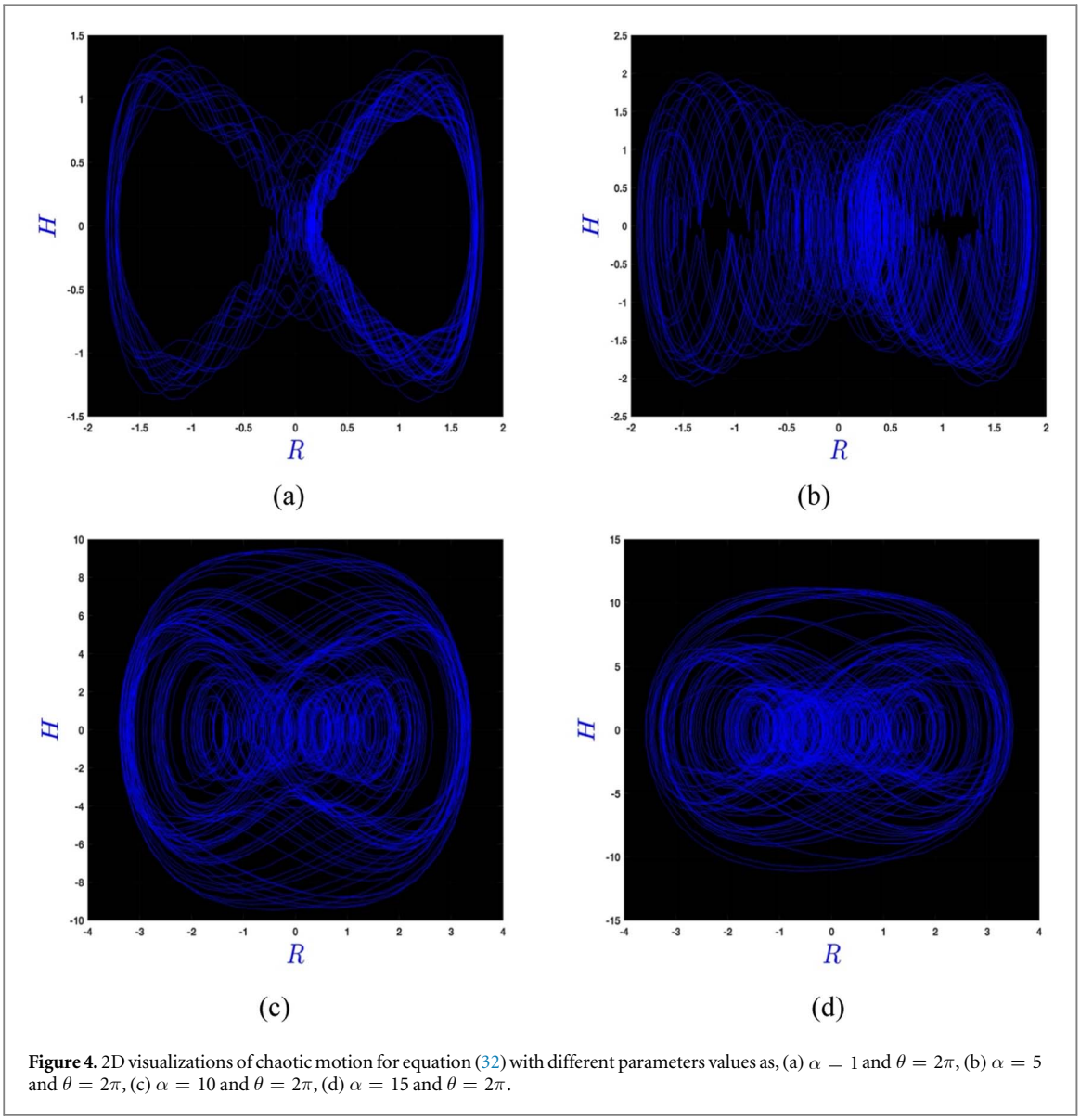

Figure 4. 2D visualizations of chaotic motion for equation (32) with different parameters values as, (a) $\alpha = 1$ and $\theta = 2\pi$, (b) $\alpha = 5$ and $\theta = 2\pi$, (c) $\alpha = 10$ and $\theta = 2\pi$, (d) $\alpha = 15$ and $\theta = 2\pi$.

Now, upon substituting these values into equation (17), which yields:

$$\mathcal{H}(\zeta) = \pm\frac{\mu\sqrt{-b}\ \sqrt{b+\varepsilon}}{2\sqrt{\kappa}}\frac{\alpha\zeta + C}{\frac{\alpha\zeta^2}{2} + C\zeta + D} \pm \frac{\mu\sqrt{-b}\ \sqrt{b+\varepsilon}\ \sqrt{C^2 - 2\alpha D}}{2\sqrt{\kappa}\frac{\alpha\zeta^2}{2} + C\zeta + D}, \tag{28}$$

where $b < 0$ and $b + \varepsilon > 0$.

Returning to its original form using transformation variables, we obtain:

$$\mathcal{H}(x,\ t) = e^{i\left(\left(\frac{-\beta^2}{(1+\epsilon\beta)}\right)x - \beta t\right)}\left(\pm\frac{\mu\sqrt{-b}\ \sqrt{b+\varepsilon}}{2\sqrt{\kappa}}\frac{\alpha(\mu(x-bt)) + C}{\frac{\alpha(\mu(x-bt))^2}{2} + C(\mu(x-bt)) + D}\right.$$
$$\left. \pm\frac{\mu\sqrt{-b}\ \sqrt{b+\varepsilon}\ \sqrt{C^2 - 2\alpha D}}{2\sqrt{\kappa}}\frac{1}{\frac{\alpha(\mu(x-bt))^2}{2} + C(\mu(x-bt)) + D}\right), \tag{29}$$

where $b < 0$ and $b + \varepsilon > 0$.

If both α and D are set to zero, but C is not equal to zero, equation (29) simplifies to as follows:

$$\mathcal{H}(x,\ t) = e^{i\left(\left(\frac{-\beta^2}{(1+\epsilon\beta)}\right)x - \beta t\right)}\left(\pm\frac{\mu\sqrt{-b}\ \sqrt{b+\varepsilon}}{\sqrt{\kappa}}\frac{1}{(\mu(x-bt))}\right), \tag{30}$$

where $b < 0$ and $b + \varepsilon > 0$.

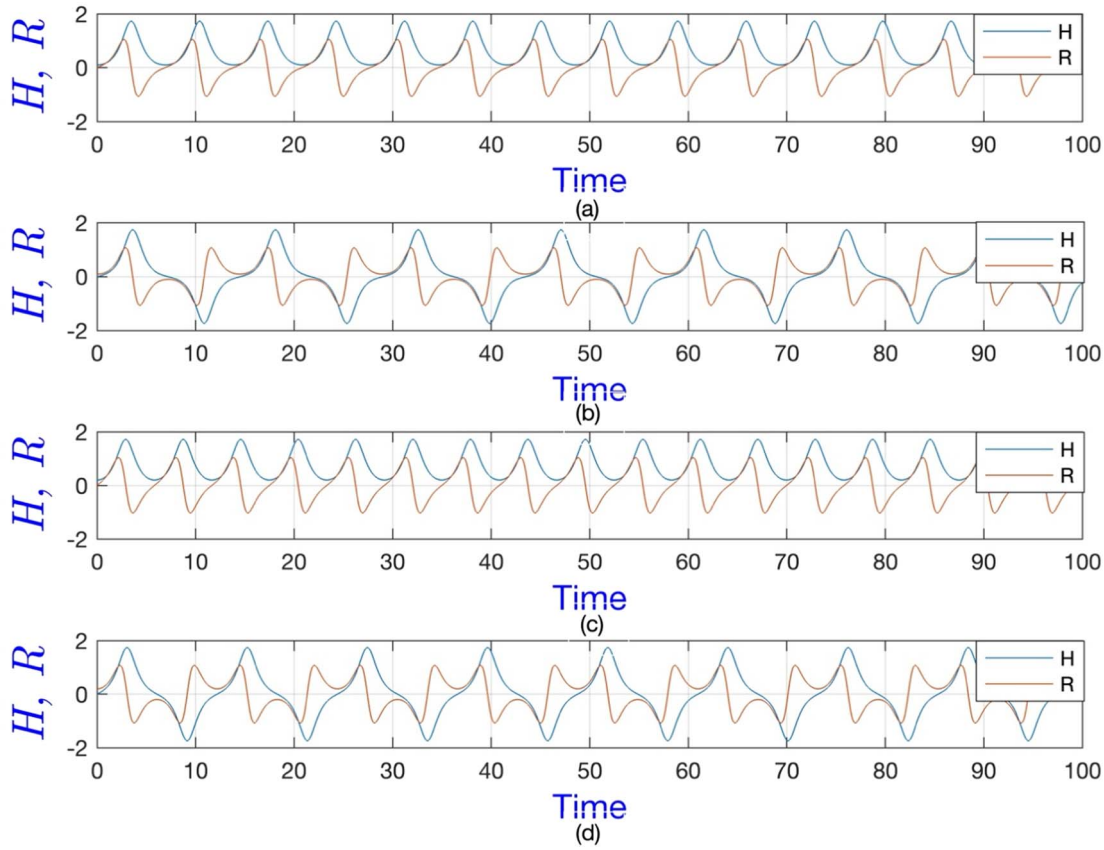

Figure 5. The state variables versus time are numerically demonstrated with initial values varying for the parameters, $k = 3$, $\mu = 1$, $\epsilon = 1$, $d = -5$, $b = 2$ and $\beta = 7$.

4. Bifurcation analysis

In this section, we conduct a crucial analysis of the governing equation known as bifurcation analysis. To do this, we attain the planar dynamical system of equation (15) as follows (Raza *et al* 2022, Rahman *et al* 2024):

$$\frac{dH}{d\zeta} = R, \quad \frac{dR}{d\zeta} = w_1 H^3 + w_2 H, \tag{31}$$

where $w_1 = \frac{-2 \quad k}{\mu^2(b^2 + \epsilon\, b)}$, and $w_2 = \frac{d + \beta^2 + d\epsilon\beta}{\mu^2(b^2 + \epsilon\, b)}$.

By introducing the Hamilton canonical equations $H' = \frac{\partial \mathcal{H}}{\partial R}$ and $R' = -\frac{\partial \mathcal{H}}{\partial H}$ in equation (31), the corresponding Hamiltonian function is as follows:

$$\mathcal{H}(H, R) = \frac{R^2}{2} - \frac{w_1 H^4}{4} - \frac{w_2 H^2}{2} = h,$$

where h is constant (Hamiltonian). To derive equilibrium points, we consider the following system of equations, $R = 0$ and $w_1 H^3 + w_2 H = 0$.

Solving this system, we obtain three equilibrium points (EPs), such as $e_1 = (0, \quad 0)$, $e_2 = \left(i\sqrt{\frac{w_2}{w_1}}, 0\right)$ and $e_3 = \left(-i\sqrt{\frac{w_2}{w_1}}, 0\right)$. The Jacobian determinant of the dynamical system:

$$D(H, R) = \begin{vmatrix} 0 & 1 \\ 3w_1 H^2 + w_2 & 0 \end{vmatrix} = -3w_1 H^2 - w_2.$$

We have three conditions for equilibrium points, (i) the equilibrium point is a saddle if $D(H, R) < 0$. (ii) the equilibrium point is a center if $D(H, R) > 0$. (iii) the equilibrium point is a cuspid if $D(H, R) = 0$.

Case 1: When, $w_1 > 0$ and $w_2 < 0$, for the choices of arbitrary constants, $k = -1$, $\mu = 1$, $\epsilon = 1$, $d = -2$, $b = -2$ and $\beta = 1$, we ascertained three equilibrium points as (0,0), (1.2247,0) and (−1.2247,0). We discovered from figure 1(a) that, (0,0) is the center point, (1.2247,0) and (−1.2247,0) both are saddle points.

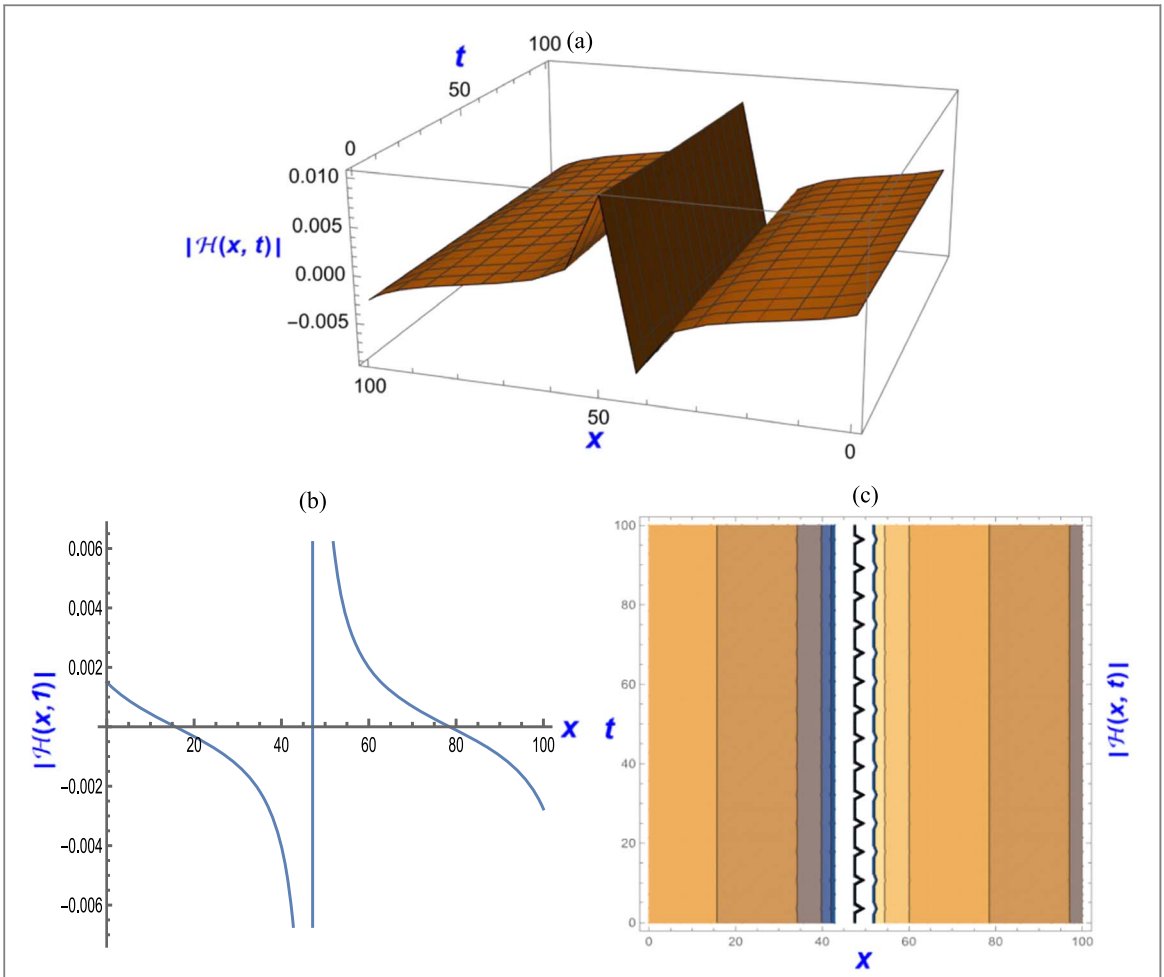

Figure 6. Graphical representations of the solutions $|\mathcal{H}(x,\ t)|$of equation (20) for $b = -.01$, $\lambda = 1$, $\varepsilon = 0.1$, $\kappa = 1$, $\mu = 0.1$, $\alpha = 1$, $C = 1$ and $D = 1$: (a) A 3D depiction (b) A 2D depiction and (c) Contour depiction.

Case 2: When, $w_1 < 0$ and $w_2 < 0$, for the choices of arbitrary constants, $k = 1$, $\mu = 1$, $\epsilon = 1$, $d = -2$, $b = 2$ and $\beta = 1$, we found one equilibrium point as (0,0). We discovered from figure 1(b) that, (0, 0) is the center point.

Case 3: When, $w_1 > 0$ and $w_2 > 0$, for the choices of arbitrary constants, $k = -1$, $\mu = 1$, $\epsilon = 1$, $d = 2$, $b = 2$ and $\beta = 1$, we found only one equilibrium point as (0,0). We discovered from figure 1(c) that, (0,0) is the saddle point.

Case 4: When, $w_1 < 0$ and $w_2 > 0$, for the choices of arbitrary constants, $k = 1$, $\mu = 1$, $\epsilon = 1$, $d = 2$, $b = -2$ and $\beta = 1$, we found three equilibrium points as (0,0), (1.5811,0) and (−1.5811,0). We discovered from figure 1(d) that, (0,0) is the saddle point, (1.5811,0) and (−1.5811,0) both are center points. All points (saddle and center) are marked in red color in all figures. These stable points (saddle and center) are very important to express many physical phenomena in optical physics and modern engineering.

5. Chaotic analysis

Here, we inserted a perturbation term in the planar dynamical system equation (31) for chaotic analysis. Let us consider the dynamical system with the perturbation term as follows (Raza *et al* 2022, Rahman *et al* 2024):

$$\frac{dH}{d\zeta} = R,\ \frac{dR}{d\zeta} = w_1 H^3 + w_2 H + \alpha\ \cos\theta(t), \tag{32}$$

where $w_1 = \frac{-2k}{\mu^2(b^2+\epsilon b)}$, and $w_2 = \frac{d+\beta^2+d\epsilon\ \beta}{\mu^2(b^2+\epsilon b)}$, $\alpha\ \cos(\theta\ \ t)$ is the perturbation term, $\alpha \neq 0$ is the amplitude of the system and $\theta \neq 0$ is the frequency of the system. We used this perturb term to explore the system's sensitivity to small changes and uncover the underlying mechanisms driving chaotic behavior. This perturbation term is known as a time-varying external forcing perturbation term. Since we focus on optical solutions context of

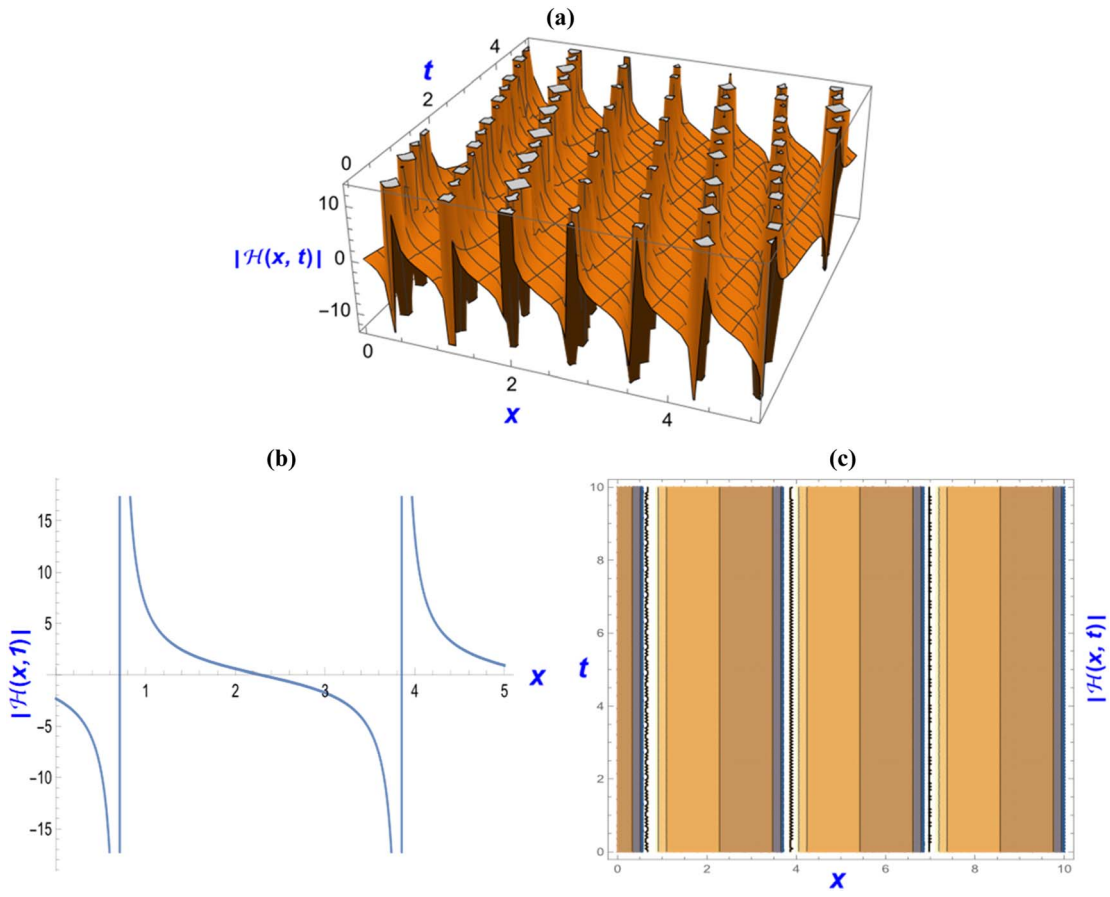

Figure 7. Graphical representations of the solutions $|\mathcal{H}(x,\ t)|$of equation (21) for $b = -.4,\ \lambda = 4,\ \varepsilon = 5,\ \kappa = 1$ and $\mu = 1$: (a) A 3D depiction (b) A 2D depiction and (c) Contour depiction.

optical solitons, perturbation terms can significantly influence their behavior. Optical solitons are localized wave packets that can maintain their shape and amplitude while propagating over long distances in certain nonlinear optical media. However, this perturbation terms play a significant role in shaping the behavior and dynamics of optical solitons, impacting their stability, interactions, and applications in nonlinear optical systems. We introduced 2D phase portraits of equation (32) with the constant values for all figures (figures 2–4) as $k = 3$, $\mu = 1$, $\epsilon = 1$, $d = -5$, $b = 2$, and $\beta = 7$. For the clear observation of the chaotic motions, we extracted phase portraits for the different values of α.

6. Sensitivity analysis

Here, we examine the sensitivity of the dynamical system described by equation (8) using the popular and effective Runge–Kutta method. To do this, we apply the Runge–Kutta method to solve the following dynamical system (Raza *et al* 2022, Rahman *et al* 2024):

$$\frac{dH}{d\zeta} = R,\ \frac{dR}{d\zeta} = w_1 H^3 + w_2 H, \tag{33}$$

The parameters have the following values, $k = 3$, $\mu = 1$, $\epsilon = 1$, $d = -5$, $b = 2$ and $\beta = 7$ and the system's initial conditions are considered by, (a) $H(0) = 0.1$ and $R = 0$; (b) $H(0) = 0$ and $R = 0.1$; (c) $H(0) = 0.2$ and $R = 0$; (d) $H(0) = 0$ and $R = 0.2$.

Figure 5 shows the outcomes that this efficient strategy produced. Class R dynamics are represented by the red curves and class H dynamics are shown by the blue curves. It is evident from the figures that even slight modifications to the starting conditions have a significant impact on the system's dynamics.

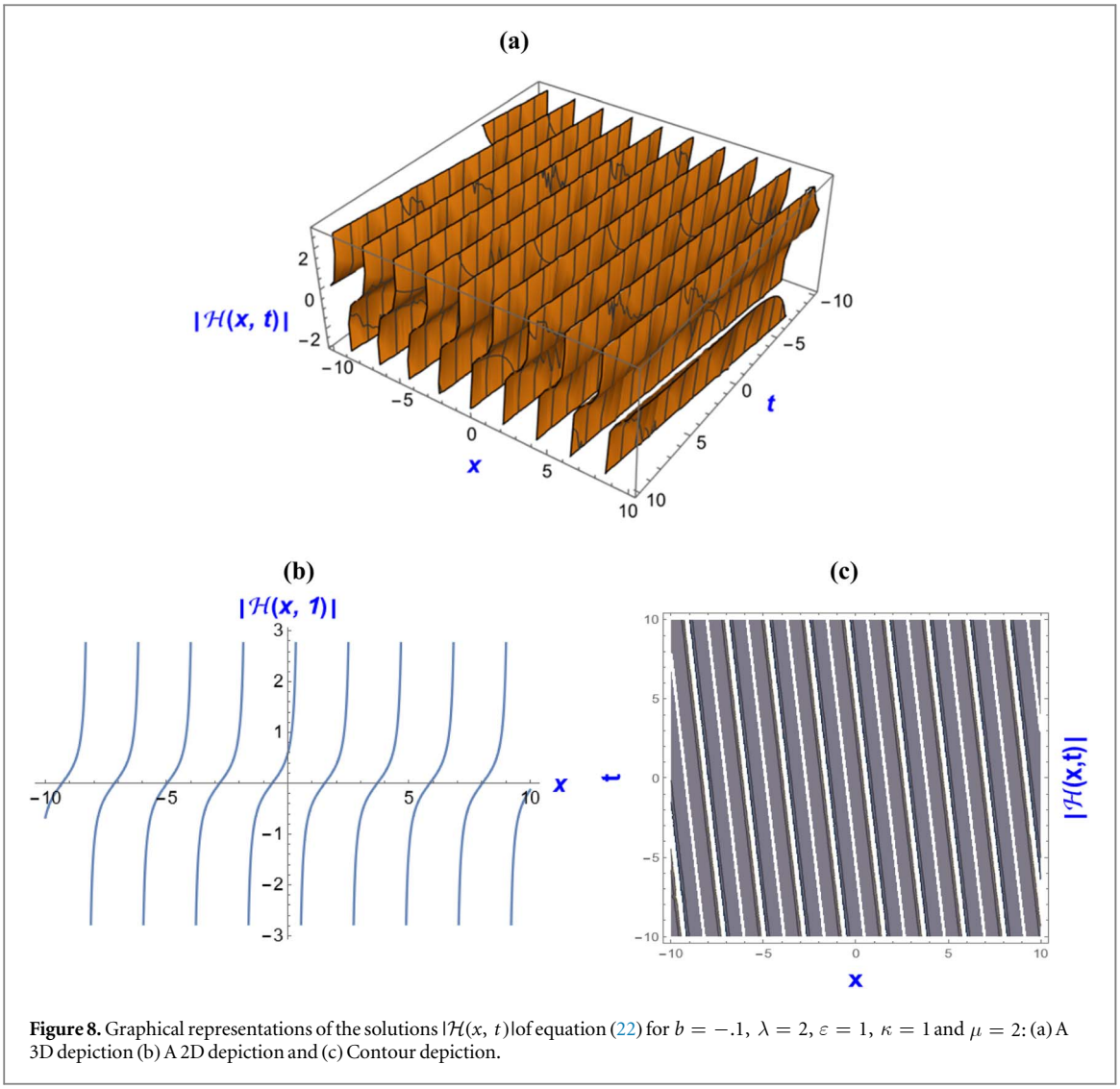

Figure 8. Graphical representations of the solutions $|\mathcal{H}(x,\ t)|$of equation (22) for $b = -.1,\ \lambda = 2,\ \varepsilon = 1,\ \kappa = 1$ and $\mu = 2$: (a) A 3D depiction (b) A 2D depiction and (c) Contour depiction.

7. Graphical representation and physical interpretations

In this segment, we leveraged the advanced computational capabilities of Mathematica to elucidate distinct graphical patterns exhibited by the HAE. Our presentation includes a variety of graphical representations, including contour plots, 2D graphics, and 3D visualizations. These depictions span a diverse range of parameter values for each relevant variable, aiming to provide a comprehensive insight into the graphical nuances of the HAE across a broad parameter space. Specific constants associated with each graph are outlined in the corresponding figure captions. Additionally, detailed discussions on various soliton types are provided for each figure.

Figure 6 is derived from equation (20) and visually shows the singular kink soliton pattern. This solution representation holds practical relevance in crafting optical components, designing fiber amplifiers, and developing nonlinear optical devices such as soliton-based frequency combs and optical switches. Additionally, the use of singular solitons proves helpful for the seamless and reliable transmission of information in optical communication systems, ensuring efficiency and stability over extended distances without succumbing to dispersion-induced distortions.

Figure 7, derived from equation (21), exemplifies one of the particular solutions stemming from equation (20), effectively showcasing the solutions' inherent multi-periodic kink characteristics. In optical physics, a multi-periodic kink is seen as a waveform with multiple kink-like shapes appearing within one period. These intricate patterns arise from complex interactions within the optical medium, like self-focusing and spatial modulation. Multi-periodic kinks can represent localized wave packets or waveguide modes with complex spatial variations, presenting potential applications in optical communication and signal processing. Understanding these phenomena thoroughly is vital for utilizing their potential in nonlinear optics and advancing optical technology.

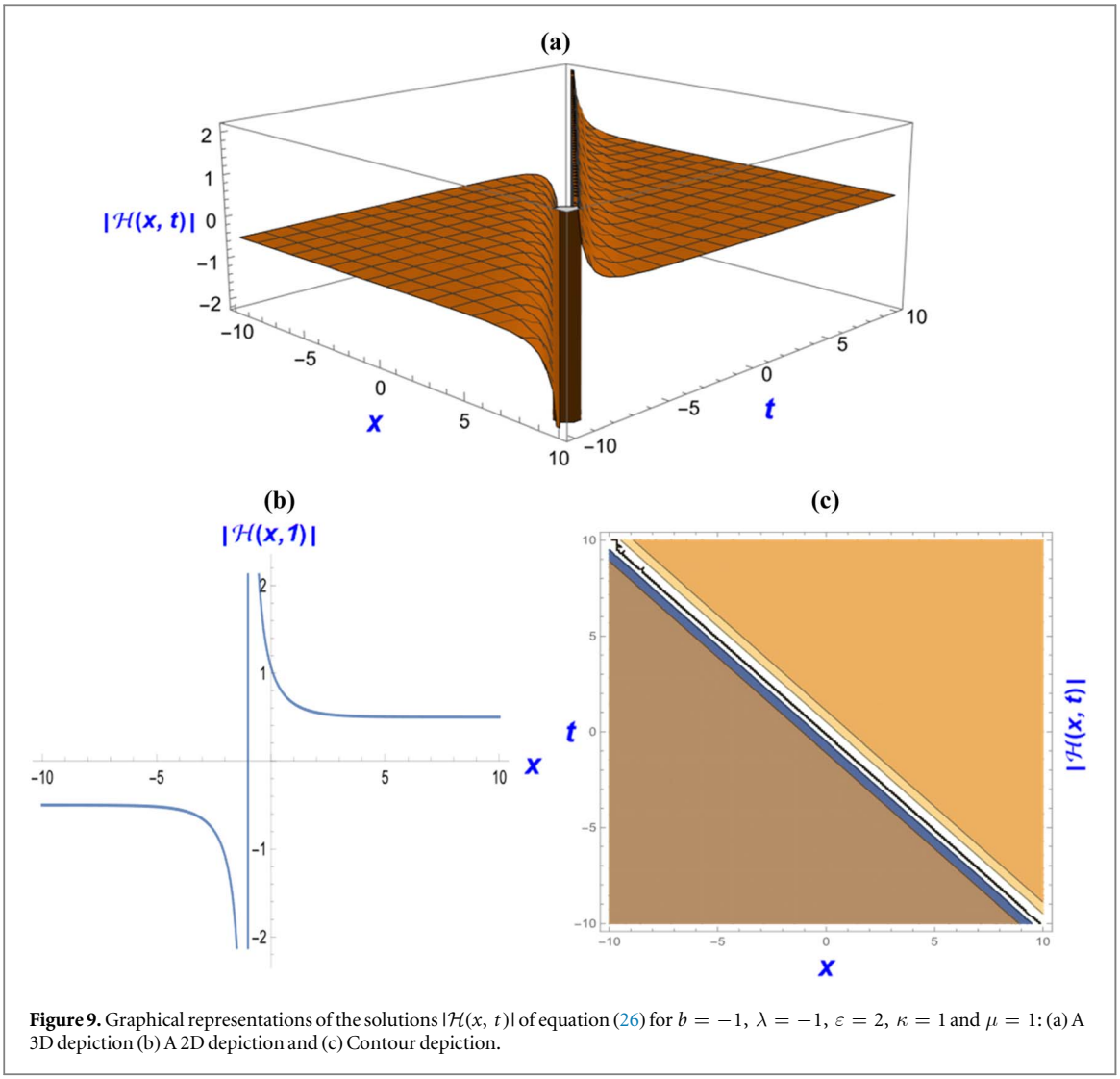

Figure 9. Graphical representations of the solutions $|\mathcal{H}(x,\ t)|$ of equation (26) for $b = -1,\ \lambda = -1,\ \varepsilon = 2,\ \kappa = 1$ and $\mu = 1$: (a) A 3D depiction (b) A 2D depiction and (c) Contour depiction.

Figure 8, arising from equation (22), illustrates a specific solution derived from equation (20), effectively highlighting the solutions' inherent singular multi-periodic behavior. Solitons featuring intricate periodic behavior offer potential applications in nonlinear frequency conversion, fiber sensors, and cutting-edge optical imaging techniques. Their distinctive properties pave the way for advancements across diverse optical technologies, underscoring their versatility and substantial impact on the field.

Figure 9, generated from equation (26), portrays a particular solution obtained from equation (25), effectively emphasizing singular kink soliton characteristics with singularity. These solitons have potential applications in optical physics, playing a crucial role in signal processing, fiber amplifiers, and ensuring stable information transmission within optical communication systems. Their significance lies in contributing to the advancement of optical technologies.

Figure 10, derived from equation (30), depicts a specific solution derived from equation (29), effectively highlighting a semi-bell-shaped pattern with singularity characterized by a specific periodicity. In the field of optical physics, the semi-bell-shaped pattern with a singularity soliton denotes a focused wave packet characterized by high localized energy. This unique pattern arises due to strong nonlinear interactions occurring within the optical medium, where the singularity soliton component significantly influences the formation of a distinct peak in intensity. These optical phenomena have wide-ranging implications across various applications, including optical communication, signal processing, and laser physics. They offer promising pathways for technological progress and furthering our understanding of the fundamental relationship between light and matter.

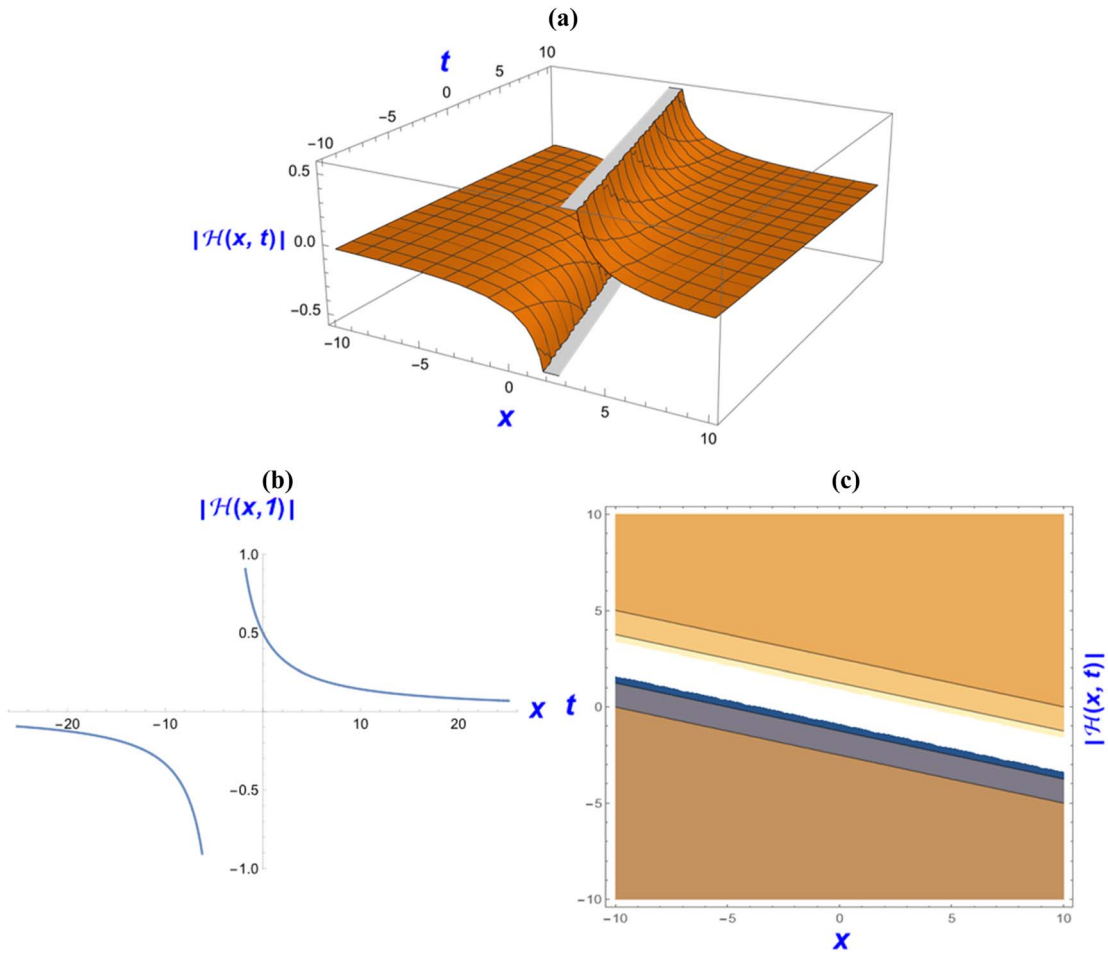

Figure 10. Graphical representations of the solutions $|\mathcal{H}(x,\ t)|$ of equation (30) for $b = -4$, $\varepsilon = 5$, $\kappa = 1$ and $\mu = 3$: (a) A 3D depiction (b) A 2D depiction and, (c) A Contour depiction.

8. Comparison

In this section, we delve into the novelty and scientific contributions of our paper through a comparative analysis of the findings presented by (Badshah *et al* 2023). This comparison is structured into two distinct sections, meticulously examining the parallels and disparities between our respective studies. By elucidating both the commonalities and divergences, we aim to provide a comprehensive understanding of the unique insights offered by our research in relation to existing literature.

8.1. Commonalities

a. Both studies center on the HAE, a crucial nonlinear complex model employed to analyze wave packet dynamics, particularly phenomena such as soliton propagation and interactions.

b. Both studies aim to obtain precise exact solutions by employing analytical techniques.

8.2. Dissimilarity and uniqueness

a. (Badshah *et al* 2023) utilized a one-variable method to obtain exact solutions, while this study employs a two-variable method ($(\dot{G}/G, 1/G)$-expansion technique).

b. This study incorporates analyses of chaotic behavior, bifurcations, and sensitivity, which were not included in (Badshah *et al* 2023) 's study.

c. While they exclusively obtain singular and periodic bell-shaped solitons, this study encompasses a broader range, including kink, multi-kink, semi-bell shape, periodic, and singular solitons.

d. This study presents a more diverse range of graphical representations, including 2D, 3D, and contour plots of exact solutions, as well as chaotic visualization, phase diagrams, and sensitivity diagrams with respect to time. In contrast, (Badshah *et al* 2023) utilized only 3D and 2D diagrams.

e. While our study places significant emphasis on the physical interpretation of diverse solitons within the context of optical physics, this aspect was not emphasized in the work by (Badshah *et al* 2023).

9. Conclusion

An application of the double $(\dot{G}/G, 1/G)$-expansion technique technique has led to the successful derivation of a diverse set of exact optical solutions for the HAE, a fundamental model governing optical soliton dynamics within optical fiber theory. Our analytical study is focused on exploring various nonlinear wave structures within the model equation, resulting in the generation of novel traveling pulse responses. These solutions possess versatile forms, such as trigonometric, hyperbolic, and rational functions.

The complex dynamics of the equation has been revealed through a methodical derivation of the related dynamical system via the Galilean transformation, together with a careful examination of bifurcation processes and chaotic behavior utilizing planar dynamical system theory. The stability of the solutions was effectively demonstrated by conducting sensitivity analysis, which was carried out using the Runge–Kutta method, even in the face of slight variations in the beginning circumstances. Also, these stable solutions encompass a wide range of behaviors, including single periodic, multi-periodic, singular soliton, and semi-bell-shaped patterns, across various values of the relevant variables. We firmly assert that those newly uncovered optical solutions hold great promise in the progression of optical physics, with implications for both light and electron optics. Notably, the optical soliton solutions derived from this method underscore its efficacy, reliability, and simplicity when compared to solutions by various alternative techniques with bifurcation and sensitivity analysis, which are more attractive to modern researchers.

This research illuminates the potential of the mentioned technique in unraveling intricate optical phenomena and contributes valuable insights into the broader domain of optical physics. The novel findings in this study provide valuable contributions to the understanding of nonlinear dynamic phenomena. Utilizing the diverse range of soliton solutions serves as a versatile toolset applicable to various aspects of optical physics. These advancements hold promise for driving progress in telecommunications, signal processing, nonlinear optics, and optical imaging.

Acknowledgments

The authors express their gratitude to researchers supporting project number (RSPD2024R535), King Saud University, Riyadh, Saudi Arabia.

Data availability statement

All data that support the findings of this study are included within the article (and any supplementary files).

Declarations

Author statement

Md Nur Hossain, Faisal Z Duraihem and Sadique Rehman: Conceptualization, Methodology, Investigation, Writing-Original draft preparation, Programming. **M Mamun Miah and Wen-Xiu Ma:** Programming, Investigating, Supervision, Writing-Reviewing and Editing.

Funding

Not applicable.

Data availability

This article contains all of the data created or examined during this investigation.

Conflict of interest

No conflicting interests have been revealed by the writers.

ORCID iDs

Md Nur Hossain https://orcid.org/0000-0002-5001-6188
M Mamun Miah https://orcid.org/0009-0007-1211-7897
Wen-Xiu Ma https://orcid.org/0000-0001-5309-1493

References

Abdel-Gawad H I and Osman M 2015 On shallow water waves in a medium with time-dependent dispersion and nonlinearity coefficients *J. Adv. Res.* **6** 593–9
Abdel-Gawad H I and Osman M S 2013 On the variational approach for analyzing the stability of solutions of evolution equations *Kyungpook Math. J.* **53** 661–80
Akbar M A, Abdullah F A and Khatun M M 2023 Optical soliton solutions to the time-fractional Kundu–Eckhaus equation through the $(G'/G, 1/G)$ -expansion technique *Opt. Quantum Electron.* **55** 1–17
Akher Chowdhury M, Mamun Miah M, Shahadat Ali H M, Chu Y M and Osman M S 2021 An investigation to the nonlinear $(2+1)$-dimensional soliton equation for discovering explicit and periodic wave solutions *Results Phys.* **23** 104013
Ali H M S, Habib M A, Miah M M, Miah M M and Akbar M A 2023 Diverse solitary wave solutions of fractional order Hirota-Satsuma coupled KdV system using two expansion methods *Alexandria Eng. J.* **66** 1001–14
Ali K K, Osman M S and Abdel-Aty M 2020 New optical solitary wave solutions of Fokas-Lenells equation in optical fiber via Sine-Gordon expansion method *Alexandria Eng. J.* **59** 1191–6
Badshah F, Alhefthi R, Tariq K U, Inc M and Kazmi S M R 2023 Some new wave solutions and modulation instability of a Hamiltonian amplitude equation in optical fibres *Optik (Stuttg.)* **291** 171327
Bekir A and San S 2012 The functional variable method to some complex nonlinear evolution equations *J. Mod. Math. Front. Sept* **1** 5–9
Biswas A 2018 Optical soliton perturbation with Radhakrishnan–Kundu–Lakshmanan equation by traveling wave hypothesis *Optik (Stuttg.)* **171** 217–20
Buckwar E and Luchko Y 1998 Invariance of a partial differential equation of fractional order under the lie group of scaling transformations *J. Math. Anal. Appl.* **227** 81–97
Cveticanin L 2006 Homotopy-perturbation method for pure nonlinear differential equation *Chaos Solitons Fractals* **30** 1221–30
Fan E 2000 Extended tanh-function method and its applications to nonlinear equations *Phys. Lett.* A **277** 212–8
Fan E and Zhang H 1998 A note on the homogeneous balance method *Phys. Lett. Sect. A Gen. At. Solid State Phys.* **246** 403–6
Fokas A S and Lenells J 2012 The unified method: I. Nonlinearizable problems on the half-line *J. Phys. A: Math. Theor.* **45** 195201
Gao W, Rezazadeh H, Pinar Z, Baskonus H M, Sarwar S and Yel G 2020 Novel explicit solutions for the nonlinear Zoomeron equation by using newly extended direct algebraic technique *Opt. Quantum Electron.* **52** 1–13
Habib M A, Ali H M S, Miah M M and Akbar M A 2019 The generalized Kudryashov method for new closed form traveling wave solutions to some NLEEs *AIMS Math* **4** 896–909
Hossain M N, Miah M M, Duraihem F Z and Rehman S 2024a Stability, modulation instability, and analytical study of the confirmable time fractional Westervelt equation and the Wazwaz Kaur Boussinesq equation *Opt. Quantum Electron.* **56** 1–29
Hossain M N, Miah M M, Hamid A and Osman G M S 2024b Discovering new abundant optical solutions for the resonant nonlinear Schrödinger equation using an analytical technique. *Opt. Quantum Electron.* **56** 847
Inan I E, Ugurlu Y and Inc M 2015 New applications of the $(G'/G, 1/G)$-expansion method *Acta Phys. Pol.* A **128** 245–51
Iqbal M A, Baleanu D, Miah M M, Ali H M S, Alshehri H M and Osman M S 2023 New soliton solutions of the mZK equation and the Gerdjikov-Ivanov equation by employing the double $G'/G,1/G$-expansion method *Results Phys.* **47** 106391
Islam S, Khan K and Arnous A H 2015 Generalized Kudryashov method for solving some *New Trends Math. Sci.* **57** 46–57
Islam S M R, Arafat S M Y and Wang H 2023 Abundant closed-form wave solutions to the simplified modified camassa-holm equation *J. Ocean Eng. Sci.* **8** 238–45
Islam S M R, Khan S, Arafat S M Y and Akbar M A 2022 Diverse analytical wave solutions of plasma physics and water wave equations *Results Phys.* **40** 105834
Jafari H, Kadkhoda N and Baleanu D 2015 Fractional Lie group method of the time-fractional Boussinesq equation *Nonlinear Dyn.* **81** 1569–74
Khan K, Salam M A, Mondal M and Akbar M A 2023 Construction of traveling wave solutions of the $(2+1)$-dimensional modified KdV-KP equation *Math. Methods Appl. Sci.* **46** 2042–54
Kumar A and Pankaj R D 2015 Tanh–coth scheme for traveling wave solutions for Nonlinear Wave Interaction model *J. Egypt. Math. Soc.* **23** 282–5
Kumar D, Hosseini K and Samadani F 2017 The sine-Gordon expansion method to look for the traveling wave solutions of the Tzitzéica type equations in nonlinear optics *Optik (Stuttg.)* **149** 439–46
Kumar S, Singh K and Gupta R K 2012 Coupled higgs field equation and hamiltonian amplitude equation: lie classical approach and (G'/G)-expansion method *Pramana - J. Phys.* **79** 41–60
Liu J G, Eslami M, Rezazadeh H and Mirzazadeh M 2019 Rational solutions and lump solutions to a non-isospectral and generalized variable-coefficient kadomtsev–petviashvili equation *Nonlinear Dyn.* **95** 1027–33

Ma W X 2021 N -soliton solutions and the Hirota conditions in (1 + 1) -dimensions *International Journal of Nonlinear Sciences and Numerical Simulation* **23** 123–33
Ma W X 2020 N-soliton solutions and the Hirota conditions in (2+1)-dimensions *Opt. Quantum Electron.* **52** 1–12
Ma W X, Huang T and Zhang Y 2010 A multiple exp-function method for nonlinear differential equations and its application *Phys. Scr.* **82** 065003
Ma W X and Lee J H 2009 A transformed rational function method and exact solutions to the 3 + 1 dimensional Jimbo-Miwa equation *Chaos Solitons Fractals* **42** 1356–63
Ma W X and Zhu Z 2012 Solving the (3 + 1)-dimensional generalized KP and BKP equations by the multiple exp-function algorithm *Appl. Math. Comput.* **218** 11871–9
Mamun A-A-, Ananna S N, An T, Asaduzzaman M and Miah M M 2022 Solitary wave structures of a family of 3D fractional WBBM equation via the tanh–coth approach *Partial Differ. Equations Appl. Math.* **5** 100237
Manafian J 2016 Optical soliton solutions for Schrödinger type nonlinear evolution equations by the tan(Pdbl(ξ)/2)-expansion method *Optik (Stuttg)* **127** 4222–45
Miah M M, Ali H M S, Akbar M A and Wazwaz A M 2017 Some applications of the (G′/G, 1/G)-expansion method to find new exact solutions of NLEEs *Eur. Phys. J. PLUS* **132** 132 252
Miah M M, Seadawy A R, Ali H M S and Akbar M A 2020 Abundant closed form wave solutions to some nonlinear evolution equations in mathematical physics *J. Ocean Eng. Sci.* **5** 269–78
Mirzazadeh M 2015 Topological and non-topological soliton solutions of Hamiltonian amplitude equation by He's semi-inverse method and ansatz approach *J. Egypt. Math. Soc.* **23** 292–6
Mirzazadeh M 2014 Modified simple equation method and its applications to nonlinear partial differential equations *Inf. Sci. Lett.* **3** 1–9
Mohanty S K, Kravchenko O V, Deka M K, Dev A N and Churikov D V 2023 The exact solutions of the 2+1–dimensional Kadomtsev–Petviashvili equation with variable coefficients by extended generalized [Formula presented]-expansion method *J. King Saud Univ. - Sci.* **35** 102358
Parkes E J and Duffy B R 1996 An automated tanh-function method for finding solitary wave solutions to non-linear evolution equations *Comput. Phys. Commun.* **98** 288–300
Rahman M, Sun M, Boulaaras S and Baleanu D 2024 Bifurcations, chaotic behavior, sensitivity analysis, and various soliton solutions for the extended nonlinear Schrödinger equation *Bound. Value Probl.* **2024** 15
Rasid M M, Miah M M, Ganie A H, Alshehri H M, Osman M S and Ma W X 2023 Further advanced investigation of the complex Hirota-dynamical model to extract soliton solutions *Mod. Phys. Lett.* B 24500741–18
Raza N, Aslam M R and Rezazadeh H 2019 Analytical study of resonant optical solitons with variable coefficients in Kerr and non-Kerr law media *Opt. Quantum Electron.* **51** 1–12
Raza N, Seadawy A R, Arshed S and Rafiq M H 2022 A variety of soliton solutions for the Mikhailov-Novikov-Wang dynamical equation via three analytical methods *J. Geom. Phys.* **176** 104515
Roshid H O, Kabir M R, Bhowmik R C and Datta B K 2014 Investigation of solitary wave solutions for vakhnenko-parkes equation via exp-function and Exp(−ϕ(ξ))-expansion method *Springerplus* **3** 692
Salas A H and Gmez S C A 2010 Application of the cole-hopf transformation for finding exact solutions to several forms of the seventh-order kdv equation *Math. Probl. Eng.* **2010** 1–15
Seadawy A R 2015 Approximation solutions of derivative nonlinear Schrödinger equation with computational applications by variational method *Eur. Phys. J. Plus* **130** 1–10
Shahzad T, Baber M Z, Ahmad M O, Ahmed N, Akgül A, Ali S M, Ali M and El Din S M 2023 On the analytical study of predator–prey model with Holling-II by using the new modified extended direct algebraic technique and its stability analysis *Results Phys.* **51** 106677
Taghizadeh N and Mirzazadeh M 2011 The first integral method to some complex nonlinear partial differential equations *J. Comput. Appl. Math.* **235** 4871–7
Tandel P, Patel H and Patel T 2022 Tsunami wave propagation model: a fractional approach *J. Ocean Eng. Sci.* **7** 509–20
Tariq K U, Younis M, Rezazadeh H, Rizvi S T R and Osman M S 2018 Optical solitons with quadratic-cubic nonlinearity and fractional temporal evolution *Mod. Phys. Lett.* B **32** 1–13
Teh C G R, Koo W K and Lee B S 1997 Jacobian elliptic wave solutions for the Wadati-Segur-Ablowitz equation *Int. J. Mod. Phys.* B **11** 2849–54
Vivas-Cortez M, Akram G, Sadaf M, Arshed S, Rehan K and Farooq K 2023 Traveling wave behavior of new (2+1)-dimensional combined KdV–mKdV equation *Results Phys.* **45** 106244
Wadati M, Segur H and Ablowitz M J 1992 A new Hamiltonian amplitude equation governing modulated wave instabilities *J. Phys. Soc. Japan* **61** 1187–93
Wang M, Li X and Zhang J 2008 The (frac(G′, G))-expansion method and travelling wave solutions of nonlinear evolution equations in mathematical physics *Phys. Lett. Sect. A Gen. At. Solid State Phys.* **372** 417–23
Wang M, Zhou Y and Li Z 1996 Application of a homogeneous balance method to exact solutions of nonlinear equations in mathematical physics *Phys. Lett. Sect. A Gen. At. Solid State Phys.* **216** 67–75
Yomba E 2005 The general projective riccati equations method and exact solutions for a class of nonlinear partial differential equations *Chinese J. Phys.* **43** 991–1003
Yuan W, Lin J and Ding J 2011 Bäcklund transformation and new exact solutions of the Sharma-Tasso-Olver equation. *Abstr. Appl. Anal.* **2011** 935710
Yue X, Kaplan M, Kaabar M K A and Yang H 2023 Exploring new features for the (2+1)-dimensional Kundu-Mukherjee-Naskar equation via the techniques of (G′/G,1/G)-expansion and exponential rational function Xiao-Guang *Opt. Quantum Electron.* **55** 97
Zafar A, Raheel M, Ali K K and Razzaq W 2020 On optical soliton solutions of new Hamiltonian amplitude equation via Jacobi elliptic functions *Eur. Phys. J. Plus* **135** 1–17
Zayed E M E and Alurrfi K A E 2014 The (G′/G, 1/G)-expansion method and its applications for solving two higher order nonlinear evolution equations *Math. Probl. Eng.* **2014** 1–20
Zayed E M E and Gepreel K A 2009 Some applications of the fenced(frac(G′, G))-expansion method to non-linear partial differential equations *Appl. Math. Comput.* **212** 1–13
Zhang Z Y 2013 Exact traveling wave solutions of the perturbed Klein-Gordon equation with quadratic nonlinearity in (1+1)-dimension, Part I. Without local inductance and dissipation effect *Turkish J. Phys.* **37** 259–67
Zhou Z J, Fu J Z and Li Z B 2006 An implementation for the algorithm of Hirota bilinear form of PDE in the Maple system *Appl. Math. Comput.* **183** 872–7